Supramolecular Chemistry, January–March 2005 Vol. 17 (1–2), pp. 173–180

Taylor & Francis
Taylor & Francis Group

Self-assembly of Resorcinarene-stabilized Gold Nanoparticles: Influence of the Macrocyclic Headgroup

BEOMSEOK KIM[a], R. BALASUBRAMANIAN[a], WALESKA PÉREZ-SEGARRA[a], ALEXANDER WEI[a,*], BJÖRN DECKER[b] and JOCHEN MATTAY[b]

[a]*Department of Chemistry, Purdue University, West Lafayette, IN, USA;* [b]*Department of Chemistry, University of Bielefeld, 33501Bielefeld, Germany*

Received (in Austin, USA) 9 July 2004; Accepted 12 September 2004

Gold nanoparticles can be encapsulated by various resorcinarene derivatives and assembled into monolayer films at solvent interfaces. Surface charge plays a critical role in both nanoparticle extraction and self-assembly: the degree of monolayer formation and local two-dimensional (2D) order within the nanoparticle arrays is dependent on the chemical nature of the resorcinarene headgroup as well as the presence of other electrolytes. Cluster size distribution analysis can be used to parameterize local 2D order within the arrays in a quantitative manner, based on mean cluster sizes and fractional hexagonal close-packed (hcp) cluster formation. 2D nanoparticle arrays can also be prepared in some cases using Langmuir–Blodgett techniques. These studies demonstrate that resorcinarenes with chemisorptive headgroups promote the self-assembly of well-ordered 2D arrays.

Keywords: Calixarenes; Nanoparticles; Encapsulation; Self-assembly

INTRODUCTION

There is currently tremendous interest in using the principles of self-assembly for the construction of materials with structural features in the low to mid-nanometer (1–100 nm) size range [1]. Self-assembly methods have the potential for fabricating well-defined nanomaterials in large scale and at low cost, and can be performed in conjunction with high-resolution lithography for nanoscale patterning. Examples of two-dimensional (2D) and three-dimensional (3D) nanoparticle superlattices have increased dramatically in recent years [2,3]. 2D nanoparticle arrays have thus far yielded novel electronic properties such as nonlinear and spin-dependent transport [4–6] or tunable optical phenomena such as second-harmonic generation [7] and surface-enhanced Raman scattering [8–10], whereas 3D superlattices and colloidal crystals are promising candidates for photonic band gaps at visible and near-infrared wavelengths [11,12].

An attractive feature of self-assembly is its ability to promote crystalline order in two or three dimensions, enabling ensemble properties to be correlated with tunable physical parameters such as particle size and aspect ratio, periodicity and interparticle spacing, and higher-order lattice structure. These scalable effects are the quintessence of nanoscale science and technology — quantized physical phenomena once considered the domain of atoms and molecules are now observed in many types of nanomaterials, giving rise to the concept of nanocrystals and their ordered superlattices as "artificial atoms" and "quantum dot solids" [2]. Nanosized logic circuits [13,14], chemical and biomolecular sensors [1,15–17] and ultradense data storage devices [18] have all been envisioned as technologically useful products created by the ordering of nanoscale components.

The forces that drive colloidal self-assembly depend on the physical characteristics and surface chemistry of the unit particle as well as on environmental factors. Particle size and composition determine whether long-range van der Waals (vdW) interactions play an important role in self-organization. For the very smallest nanoparticles, such vdW forces are typically at or below thermal energies (k_BT), such that self-assembly would be mostly driven by interactions at molecular length

*Corresponding author. E-mail: alexwei@purdue.edu

ISSN 1061-0278 print/ISSN 1029-0478 online
DOI: 10.1080/10610270412331328961

scales (e.g. surfactant chain interdigitation) [19–21]. "Programmed" nanoparticle self-assembly mediated by molecular recognition has been demonstrated in several instances [22–28] with at least one example of ordered superlattice formation reported recently [29]. As particle size increases, self-organization is often determined by a more complex balance of vdW interactions, electrostatic forces and/or short-range steric repulsion; at still greater (mesoscopic) length scales, interfacial surface energies and solvophobic interactions become significant [30].

Not surprisingly, methods for assembling colloidal particles into ordered superlattices vary considerably, depending on the nature of the particles used and the media in which they are dispersed. Surfactant-coated nanocrystals with weak vdW interactions can be deposited at submonolayer concentrations onto air–water interfaces and compressed into close-packed 2D arrays in a Langmuir–Blodgett trough [7,19,20,31–33] or organized into 3D superlattices by molecular crystal growth techniques [34–36]. Stable dispersions of nanoparticles and colloids with greater long-range vdW interactions can self-assemble into 2D arrays by simple dropcasting techniques onto wettable surfaces [21,37–43]. Air–liquid and liquid–liquid interfaces are especially useful for tuning particle interactions, and permit self-assembled films to be transferred onto solid surfaces with a high degree of fidelity. Several examples of highly ordered 2D colloidal arrays have been prepared by Langmuir monolayer transfer [33,44,45].

With respect to metal nanoparticles, the vast majority of studies on nanoscale self-assembly have focused on particles in the low nanometer size range ($d < 10$ nm). Metal colloids in the mid-nanometer (10–100 nm) size range also have important optical or magnetic properties, but their strong interaction potentials promote kinetic aggregation and often result in poorly organized structures. This is essentially a problem in dispersion control; if repulsive interactions are sufficiently strong to offset particle self-attraction at close range, it should be possible to achieve conditions for thermodynamically controlled self-organization irrespective of particle size.

In order to tap the potential of nanomaterials in the relatively unexplored 10–100 nm size range, we have developed surfactants derived from *C*-undecylcalix[4]resorcinarene [46] to enhance both the dispersion of colloidal metal particles in various solvents and their self-assembly into well-defined nanostructures with tunable properties [10,47–55]. These compounds possess at least two salient features that contribute to their superior qualities as nanoparticle dispersants: (i) large, multivalent headgroups for robust adsorption onto the nanoparticle surface, and (ii) several

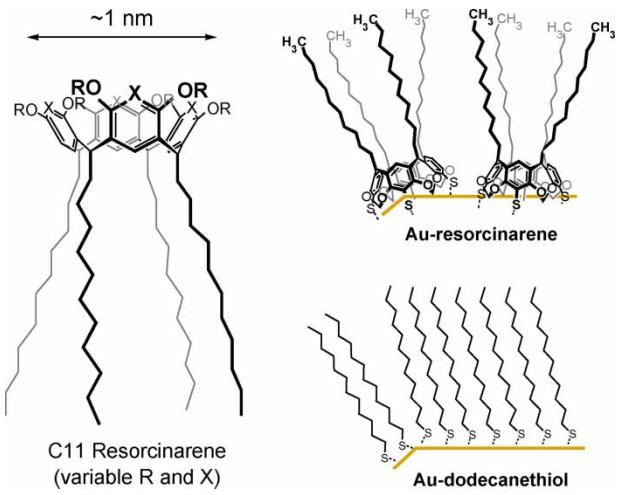

FIGURE 1 Resorcinarenes as nanoparticle surfactants. Resorcinarene monolayers support chains at intermediate packing densities (*upper right*) and retain a high degree of conformational entropy at the nanoparticle surface. Single-chain surfactants tend to assemble into monolayers with high packing densities (*lower right*) and limited potential for entropic steric repulsion.

hydrocarbon chains per molecule spaced several angstroms apart (see Fig. 1). The latter ensures a high degree of configurational freedom per chain in the surfactant layer, which translates into effective steric repulsion associated with the loss of entropy. This is particularly important for nanoparticles with planar facets or a large radius of curvature; single-chain surfactants on these particles tend to form densely packed monolayers with minimal entropic repulsive potential (see Fig. 1, *lower right*), which translates into poor kinetic control during nanoscale self-assembly [47,52].

In the course of these studies, we demonstrated that colloidal Au particles as large as 170 nm could be dispersed at the air–water interface and organized into monoparticulate films when encapsulated by resorcinarene tetrathiol **1** [50,52]. These were deposited onto planar substrates and analyzed by transmission electron microscopy (TEM), which confirmed the formation of hexagonally close-packed 2D arrays with good local order. The Au nanoparticle arrays exhibited size-tunable optical properties including surface-enhanced Raman scattering (SERS), a highly sensitive form of surface spectroscopy with exciting potential for chemical and biomolecular sensing [10]. The SERS activities of the 2D arrays was observed to be both reproducible and stable over a period of months, attributable to the thermodynamic stability of the arrays themselves.

In this article we investigate the surfactant properties of several resorcinarene-like derivatives (**1**–**8**) for nanoparticle dispersion and self-assembly (see Fig. 2). By varying the chemical functionality

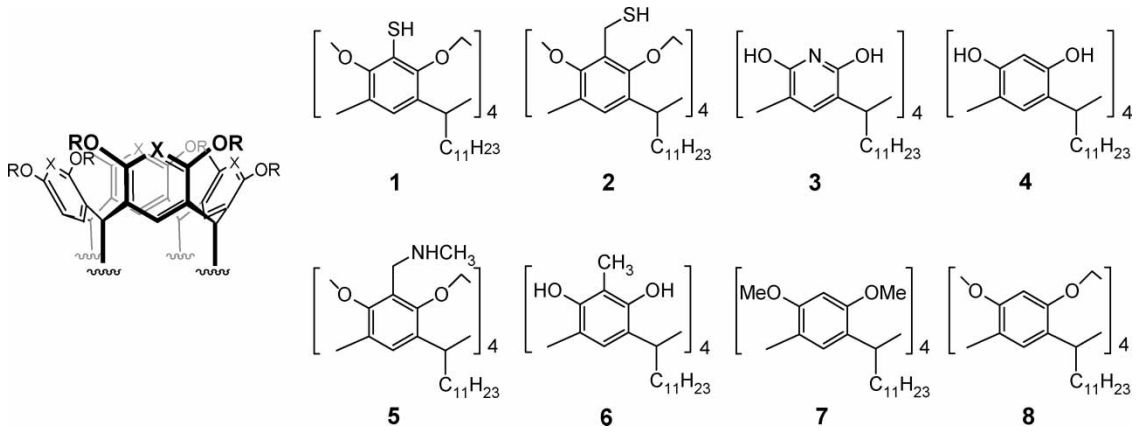

FIGURE 2 Tetra-*C*-undecylresorcinarene derivatives and related analogs. **1**: X = C–SH, R = $-CH_2-$; **2**: X = C–CH_2SH, R = $-CH_2-$; **3**: X = N, R = H; **4**: X = CH, R = H; **5**: X = C–CH_2NHCH_3, R = $-CH_2-$; **6**: X = C–CH_3, R = H; **7**: X = CH, R = OCH_3; **8**: X = CH, R = $-CH_2-$.

on the resorcinarene headgroups while keeping the hydrocarbon chains constant, we are able to evaluate chemisorption effects on nanoparticle extraction and self-organization at the air–water interface. This work complements a recent study on the influence of adsorbed electrolyte in the self-assembly and local 2D ordering of nanoparticle arrays stabilized by resorcinarene **1** [56]. Both studies demonstrate the importance of surface charge for nanoparticle self-organization at aqueous interfaces.

RESULTS AND DISCUSSION

Extraction and Self-assembly of Resorcinarene-stabilized Au Nanoparticles

Aqueous suspensions of colloidal Au nanoparticles (35 ± 3 nm, $\sim 10^{11}$ particles/mL) were first conditioned with an ion-exchange resin to reduce electrolyte concentrations to a minimum. Resorcinarene-encapsulated nanoparticles were prepared by mixing the conditioned Au nanoparticle suspension with an equal portion of a 1 mM solution of resorcinarene in THF, to produce a homogeneous pink solution (see Materials and Methods for additional details). Addition and vigorous mixing of toluene resulted in a separation of organic and aqueous layers; in many cases, a dark bluish film could be observed at the solvent interface, signifying the formation of a densely packed nanoparticle film. After removing the organic layer, the films were transferred onto carbon-coated Cu grids for TEM analysis.

Resorcinarene derivatives **1**–**4** were all capable of mediating the self-assembly of Au nanoparticles at the aqueous interface, but their efficacy depended on the condition of the aqueous medium prior to nanoparticle extraction (see Fig. 3). In particular, the presence of associative electrolytes such as NaCl and sodium citrate (Na_3Cit) played an important role in determining the efficiency of extraction. For example, Au nanoparticles suspended in solutions with minimal electrolyte ($I \ll 1$ mM) were extracted to the aqueous interface by tetraarylthiol derivative **1** and octahydroxy derivative **4**, but only partially extracted by tetraazaresorcinarene analog (pyridinearene) **3**. However, Au nanoparticles treated with tetrabenzylthiol derivative **2** were not confined to the solvent interface, but were transferred completely into the organic phase [48,49]. Raising the NaCl and Na_3Cit concentrations to millimolar levels ($I = 8.95$ mM) had a dramatic effect. In the case of tetrabenzylthiol **2**, a large fraction of encapsulated nanoparticles were not transferred into the organic layer but remained confined at the solvent interface, whereas in the case of tetraaza analog **3**, the nanoparticles were not extracted at all but remained suspended in aqueous solution. In comparison, resorcinarenes **1** and **4** remained essentially constant in their extraction efficiencies.

Two assumptions can be made based on the above observations. First, adsorbed electrolytes are not completely displaced by the resorcinarene surfactants, such that the encapsulated nanoparticles are rendered amphipathic by the residual surface charge [56]. This confines the nanoparticles to the aqueous interface and promotes their self-organization into 2D arrays, as noted in several other self-assembly studies involving functionalized latex and silica particles [44,57–60]. Second, the resorcinarenes adsorb onto the nanoparticle surfaces primarily through chemisorption rather than electrostatic interactions. In the cases of tetraazaresorcinarene analog **3** and octahydroxy derivative **4**, both

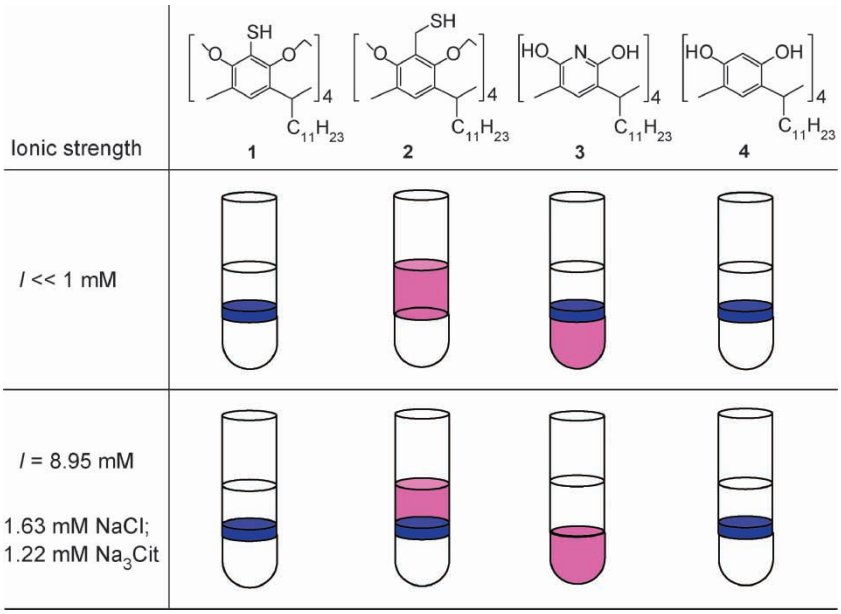

FIGURE 3 Illustrations of nanoparticle extractions by resorcinarenes **1**–**4**, in the absence and presence of aqueous electrolyte. Self-assembled nanoparticle films at the aqueous interface appeared dark blue.

of these are expected to adsorb as anions in the absence of strong acids[†,‡] [61,62]. It is worth noting that while pyridinearene **3** can extract colloidal gold nanoparticles in the presence of minimal electrolyte, attempts to extract nanoparticles using tetra(*N*-methylamino)methylresorcinarene **5** under identical conditions were unsuccessful. Furthermore, exposing extracted nanoparticles encapsulated in **3** to 0.1 M HCl resulted in their redispersion to the aqueous medium. This demonstrates that the Lewis basicity of the headgroup is important for surface adsorption.

Nanoparticles encapsulated by tetra-*C*-methylresorcinarene **6** or octa-*O*-methyl ether derivative **7** could be extracted to the aqueous interface but were not well dispersed, suggesting that the surfactant layer was not sufficiently robust against desorption to prevent rapid kinetic aggregation (see Fig. 4). We have previously shown octamethyl ether **7** to be an effective surfactant for entrapping and dispersing neutral gold nanoparticles (generated as aerosols) in hydrocarbon solutions, but this surfactant layer could be easily displaced by competing adsorbates [47]. Finally, cavitand **8** showed little ability to extract colloidal Au nanoparticles from aqueous solution and was deemed to be a poor encapsulating agent, in line with previous observations using aerosol-generated gold nanoparticles [47].

Characterization of 2D Nanoparticle Arrays

Au nanoparticle films were transferred onto carbon-coated Cu grids using Langmuir–Schaefer conditions for TEM analysis (see Fig. 4). Nanoparticles encapsulated by resorcinarenes **1**–**3** were observed to assemble into 2D arrays with good local order, demonstrative of thermodynamic self-organization. In comparison, nanoparticles encapsulated by **4** produced monoparticulate films with less order, and those encapsulated by resorcinarenes **6** and **7** resulted in multilayers. The latter experiments correlate with a loss of dispersion control, most likely related to the weaker adsorption of these surfactants to the nanoparticle surface. Surfactant desorption compromises short-range steric repulsion, permitting self-assembly to be dominated by kinetic aggregation. Overall, these results confirm that resorcinarenes with good chemisorption properties are important for promoting nanoparticle self-organization at aqueous interfaces.

In order to better characterize the quality of local 2D order within the self-assembled nanoparticle arrays, the TEM images were subjected to a quantitative method of analysis based on cluster size distributions [56]. Radial distribution ($g(r)$) functions were derived from digitally processed TEM images, and used to generate lattice parameters for the determination of hexagonal close-packed

[†]While the pK_a values of compound 3 have not been measured, it is known that 2,6-dihydroxypyridine exists in monoanionic form between pH 4.2 and 15.

[‡]The pK_a values of a water-soluble version of 4 have been measured by pH titration, with the first ionization occurring at pH 6.95: see Ref. [62].

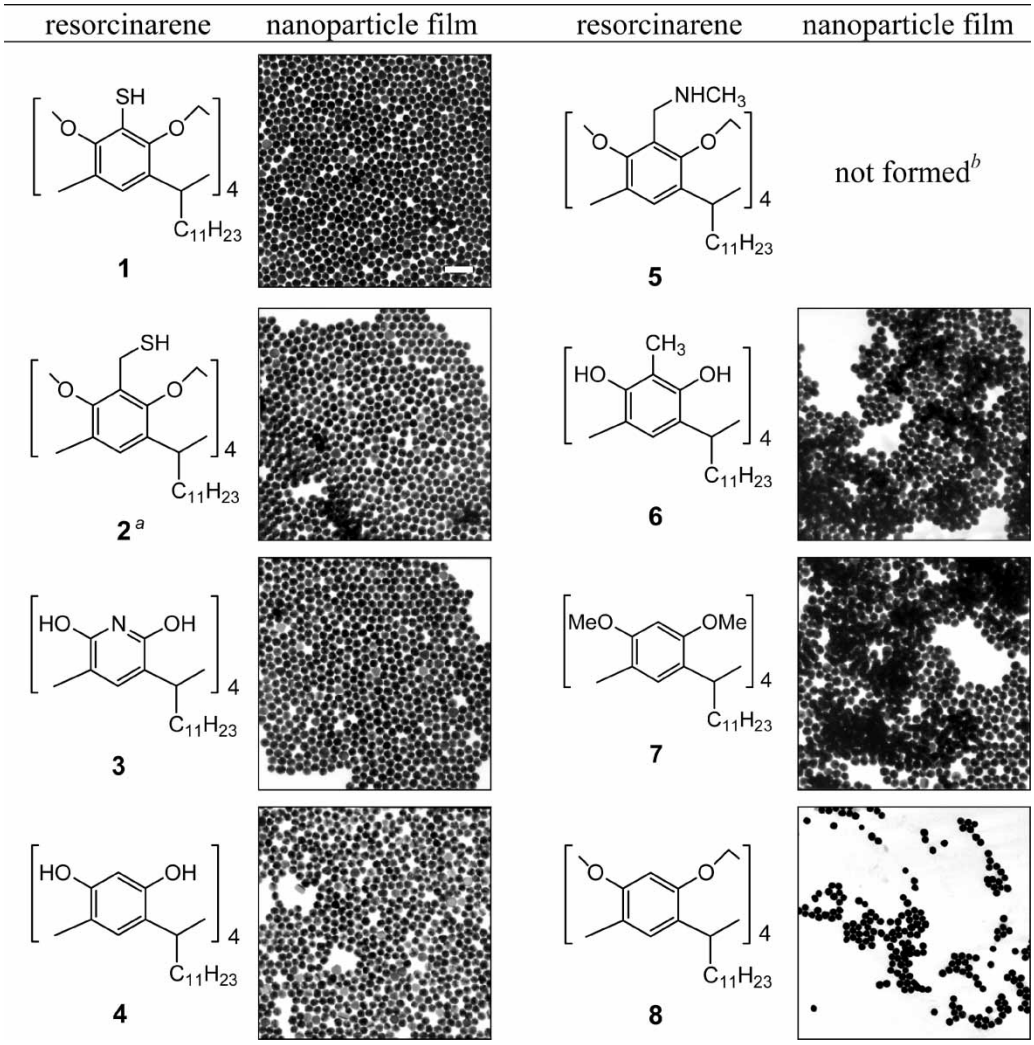

FIGURE 4 Self-assembly of resorcinarene-encapsulated Au nanoparticles (35 ± 3 nm) upon extraction to aqueous interfaces. Nanoparticle films were transferred onto carbon-coated Cu grids for TEM analysis. Scale bar = 100 nm. [a]Nanoparticles were extracted from aqueous suspensions containing electrolyte ($I = 8.95$ mM). [b]Nanoparticles remained dispersed in aqueous solution.

(hcp) arrays (see Fig. 5). Cluster size distributions were restricted to nonoverlapping domains to prevent redundancy in particle count [56]. This method enables 2D order to be described in quantitative terms, using number-averaged and weight-averaged cluster sizes (M_n and M_w, respectively) and fractional hcp values (f_{hcp}) as figures of merit.

Cluster size distribution analyses were performed on self-assembled nanoparticle films, formed upon extraction to the aqueous interface by resorcinarenes **1**–**3**. The 2D order within these films was determined to be comparable, with M_n and f_{hcp} in the range of 20 and 0.60, respectively (see Table I)[¶]. In comparison, analysis of nanoparticle films formed with resorcinarene **4** produced significantly smaller values for M_n and f_{hcp} (15.1 and 0.43, respectively). A similar loss in 2D order has been observed when nanoparticles were extracted by **1** from solutions containing additional NaCl and Na_3Cit [56]. Both results suggest that while surface-bound electrolytes can be useful for confining surfactant-encapsulated nanoparticles to aqueous interfaces, they are also capable of promoting kinetic aggregation and can have an unpredictable effect on self-assembly.

Nanoparticle Arrays by Langmuir–Blodgett Compression

Resorcinarene-stabilized nanoparticles have excellent dispersion characteristics in organic solvents, suggesting the possibility of using Langmuir–Blodgett techniques for creating 2D nanoparticle arrays [7,31–33]. In particular, nanoparticles encapsulated by tetrabenzylthiol **2** can be fully

[¶]It is worth mentioning that f_{hcp} serves as a lower limit when calculated with the assumption of nonoverlapping clusters. Values in the range of 0.70 are obtained if partially overlapping clusters (up to 30%) are allowed.

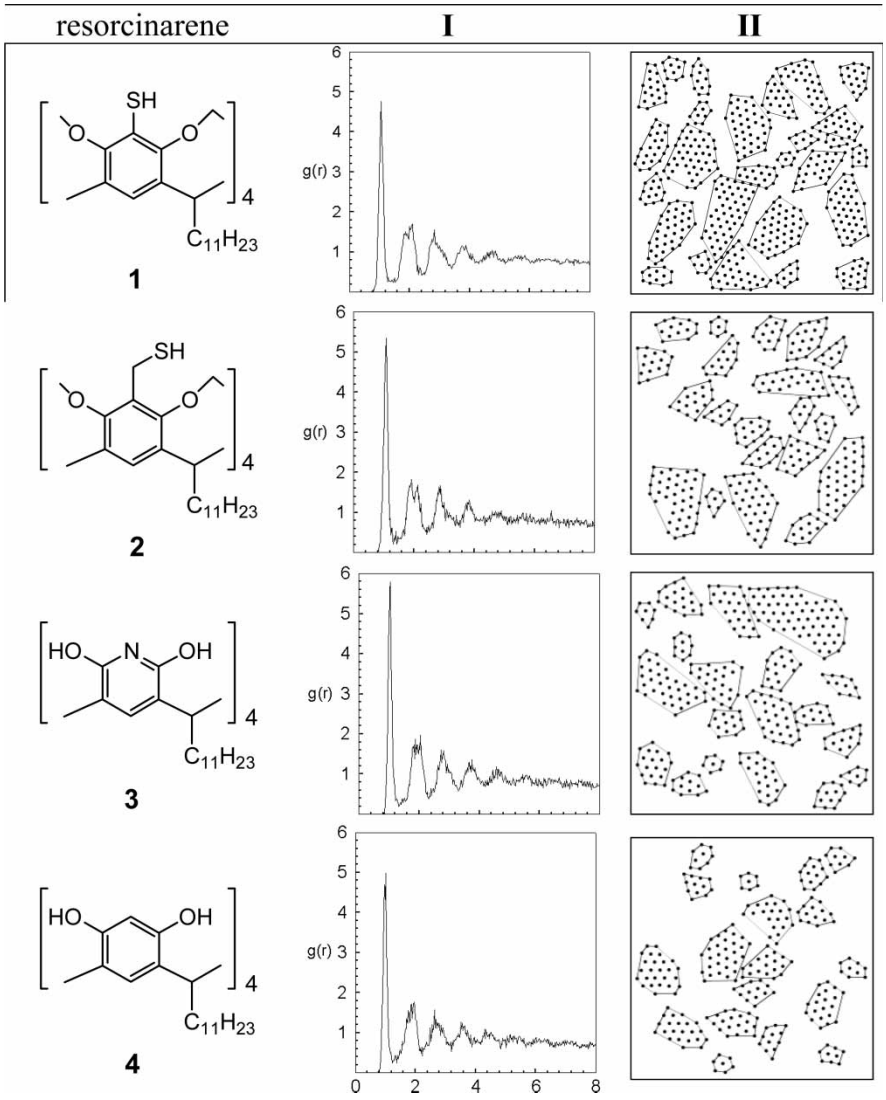

FIGURE 5 Cluster size distribution analysis of resorcinarene-encapsulated Au nanoparticle arrays, based on TEM images in Fig. 4. Column I: radial distribution functions derived from digitized images. Column II: nonoverlapping hcp clusters within self-assembled nanoparticle films. Domain boundaries are drawn to guide the eye.

extracted into the organic phase, and redeposited onto air–water interfaces [48]. However, when 35-nm Au particles encapsulated by **2** were extracted into toluene and condensed onto an aqueous interface, only multilayered films were produced. This suggests that as the residual film is concentrated, kinetic aggregation driven by the nanoparticles' vdW attractions supersedes reversible self-organization at the solvent interface.

TABLE I Cluster size distribution analysis of resorcinarene-stabilized nanoparticle arrays

			hcp clusters (nonoverlapping)		
Compound	Particle size (nm)	Particle count (N)*	M_n	M_w	f_{hcp}
1†	35 ± 3	901	21.4	28.5	0.64
2	35 ± 3	601	17.1	21.9	0.60
2‡	9.2 ± 0.8	852	18.4	22.6	0.52
3	35 ± 3	616	18.7	26.8	0.58
4	35 ± 3	640	15.1	17.9	0.43

*Number of centroids taken from TEM image (cf. Fig. 5). †Data taken from Ref. [56]. ‡Formed after compression in a Langmuir–Blodgett trough (cf. Fig. 6).

To ascertain whether particle size was responsible for poor kinetic control, the same procedure was repeated using toluene extracts of 9.2-nm Au particles. These were indeed amenable to monolayer film formation, and could be subjected to surface compression to maximize the overall packing (see Fig. 6). However, cluster size distribution analysis revealed no improvement in 2D order; the M_n and f_{hcp} values of the arrays obtained after Langmuir–Blodgett compression were no greater than those formed by self-organization under amphipathic conditions (see Table I). TEM images of 9.2-nm particle films obtained in the absence of surface compression (not shown) revealed that the particles

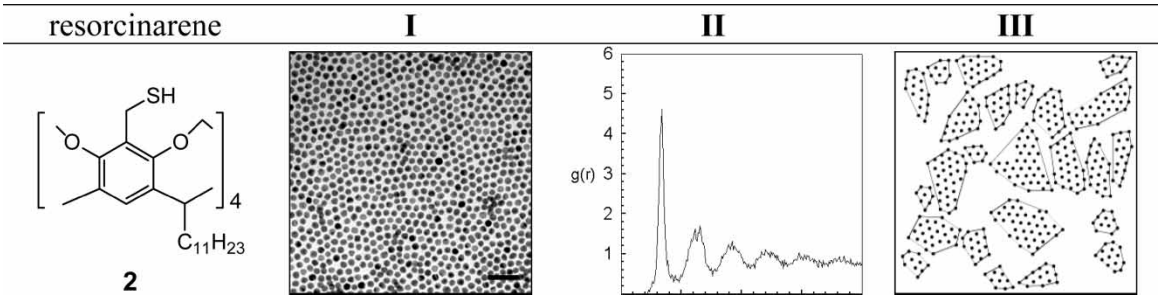

FIGURE 6 TEM image and cluster size distribution analysis of 2D arrays of 9.2-nm Au particles encapsulated by **2**, transferred after compression in a Langmuir–Blodgett trough. I: TEM image of nanoparticle film (scale bar = 50 nm); II: radial distribution functions derived from digitized images; III: nonoverlapping hcp clusters within self-assembled nanoparticle films.

were already assembled into close-packed domains, an indication that vdW forces continued to provide the dominant driving force for nanoparticle self-assembly. Thus, while resorcinarene **2** substantially enhances the dispersion of Au nanoparticles, additional repulsion potential is needed to achieve self-assembly conditions with complete thermodynamic control.

MATERIALS AND METHODS

Resorcinarene derivatives **1**, **2**, **4**–**8** and tetraazaresorcinarene analog (pyridine[4]arene) **3** were synthesized as reported previously or by a slight modification of published procedures[§,‖] [63–65]. Colloidal Au particle suspensions were purchased from British Biocell International (EM.GC10, *ca.* 5.7×10^{12} particles/mL; EM.GC40, *ca.* 9×10^{10} particles/mL) and characterized by TEM (Philips EM-400, 80 keV); the average particle sizes were 9.2 ± 0.8 nm ($N = 846$) and 35 ± 3 nm ($N = 1165$), respectively. Carbon-coated Cu TEM grids were purchased from Ted Pella, Inc. and used as supplied. The resorcinarene-encapsulated nanoparticles were handled in silanized glassware (SiliClad, Gel-Est) to minimize electrostatic surface adsorption. High-purity water with measured resistivity above 18 MΩ cm was obtained using an ultrafiltration system (Milli-Q, Millipore) equipped with an additional 0.22-μm membrane filter.

Aqueous suspensions of colloidal Au particles were treated with a mixed-bed ion-exchange resin (Amberlite MB-3, Mallinckrodt) for 30 min to remove excess electrolyte[#]. In a typical experiment, resorcinarene-encapsulated nanoparticles were prepared by vigorously mixing colloidal suspensions (1 mL) with 1 mM solution of surfactant in freshly distilled THF (1 mL) in a silanized glass tube, which resulted in a homogeneous pink solution. In the case of nanoparticles encapsulated with resorcinarene **2**, NaCl and Na_3Cit were reintroduced in controlled amounts (1.63 and 1.22 mM, respectively) prior to extraction. Addition and vigorous mixing of toluene (1 mL) resulted in a separation of organic and aqueous layers, with amphipathic nanoparticle films spontaneously assembled at the solvent interface. The organic layer was removed by pipette, and the aqueous layer and particles were washed twice more with toluene (1 mL each) to extract THF and excess surfactant. The Au nanoparticle films were drawn up in a silanized glass pipette, then drained and carefully redeposited onto a clean air–water interface in a silanized test-tube and allowed to stand at room temperature for 60 min. The nanoparticle film was then transferred onto carbon-coated Cu TEM grids by Langmuir–Schaefer transfer using a pair of forceps, and dried in air.

Nanoparticle Films by Langmuir–Blodgett Compression

An aqueous suspension of 9.2-nm Au particles (3.5 mL) was mixed was an equal portion of a 1 mM solution of resorcinarene **2** in THF, then extracted with toluene (17 mL). Encapsulated particles were treated with methanol (6 mL) and centrifuged at 6000 *g* for 20 min, then redispersed in 0.3 mL toluene with the aid of an ultrasonic cleaning bath (4 × 5-s exposures). Nanoparticle dispersions were drawn up in a silanized glass pipette, then slowly redeposited onto a clean air–water interface in a Langmuir–Blodgett trough (Nima Technologies, 611M), allowing time fo the evaporation of toluene. The resulting Au nanoparticle film was slowly compressed (barrier speed = 1 mm/min) until

[§]Compounds **1**, **2** and **6**: see Ref. [50]; compounds **4** and **7**: see Ref. [47].
[‖]Compound **3**; Compound **5**; Compound **8**.
[#]Additional experimental details can be found in Ref. [56].

the theoretical area for a monolayer was achieved. The film was transferred onto a carbon-coated Cu TEM grid using a pair of forceps, and dried in air.

Acknowledgements

We gratefully acknowledge financial support from the National Science Foundation (BES-0228143, CHE-0243496 and ECS-0210445) and the Deutsche Forschungsgemeinschaft (SFB 613).

References

[1] Shipway, A. N.; Katz, E.; Willner, I. *Chem. Phys. Chem.* **2000**, *1*, 18.
[2] Collier, C. P.; Vossmeyer, T.; Heath, J. R. *Annu. Rev. Phys. Chem.* **1998**, *49*, 371.
[3] Pileni, M. P. *J. Phys. Chem. B* **2001**, *105*, 3358.
[4] Andres, R. P.; Bielefeld, J. D.; Henderson, J. I.; Janes, D. B.; Kolagunta, V. R.; Kubiak, C. P.; Mahoney, W. J.; Osifchin, R. G. *Science* **1996**, *273*, 1690.
[5] Parthasarathy, R.; Lin, X.-M.; Jaeger, H. M. *Phys. Rev. Lett.* **2001**, *87*, 186807.
[6] Black, C. T.; Murray, C. B.; Sandstrom, R. L.; Sun, S. *Science* **2000**, *290*, 1131.
[7] Collier, C. P.; Saykally, R. J.; Shiang, J. J.; Henrichs, S. E.; Heath, J. R. *Science* **1997**, *277*, 1978.
[8] Moody, R. L.; Vo-Dinh, T.; Fletcher, W. H. *Appl. Spectrosc.* **1987**, *41*, 966.
[9] Tessier, P. M.; Velev, O. D.; Kalambur, A. T.; Rabolt, J. F.; Lenhoff, A. M.; Kaler, E. W. *J. Am. Chem. Soc.* **2000**, *122*, 9554.
[10] Wei, A.; Kim, B.; Sadtler, B.; Tripp, S. L. *Chem. Phys. Chem.* **2001**, *2*, 743.
[11] Moroz, A. *Phys. Rev. Lett.* **1999**, *83*, 5274.
[12] Braun, P. V.; Wiltzius, P. *Curr. Opin. Colloid Interface Sci.* **2002**, *7*, 116.
[13] Feldheim, D. L.; Keating, C. D. *Chem. Soc. Rev.* **1998**, *27*, 1.
[14] Smith, C. G. *Science* **1999**, *284*, 274.
[15] Wohltjen, H.; Snow, A. W. *Anal. Chem.* **1998**, *70*, 2856.
[16] Krasteva, N.; Besnard, I.; Guse, B.; Bauer, R. E.; Mullen, K.; Yasuda, A.; Vossmeyer, T. *Nano Lett.* **2002**, *2*, 551.
[17] Genov, D. A.; Sarychev, A. K.; Shalaev, V. M.; Wei, A. *Nano Lett.* **2004**, *4*, 153.
[18] Chou, S. Y.; Krauss, P. R.; Kong, L. *J. Appl. Phys.* **1996**, *79*, 6101.
[19] Heath, J. R.; Knobler, C. M.; Leff, D. V. *J. Phys. Chem. B* **1997**, *101*, 189.
[20] Gelbart, W. M.; Sear, R. P.; Heath, J. R.; Chaney, S. *Faraday Discuss.* **1999**, *112*, 299.
[21] Motte, L.; Pileni, M. P. *J. Phys. Chem. B* **1998**, *102*, 4104.
[22] Mirkin, C. A.; Letsinger, R. L.; Mucic, R. C.; Storhoff, J. J. *Nature* **1996**, *382*, 607.
[23] Storhoff, J. J.; Mirkin, C. A. *Chem. Rev.* **1999**, *99*, 1849.
[24] Alivisatos, A. P.; Johnsson, K. P.; Peng, X.; Wilson, T. E.; Loweth, C. J.; Bruchez, M. P. Jr.; Schultz, P. G. *Nature* **1996**, *382*, 609.
[25] Cusack, L.; Rizza, R.; Gorelov, A.; Fitzmaurice, D. *Angew. Chem., Int. Ed. Engl.* **1997**, *36*, 848.
[26] Liu, J.; Mendoza, S.; Roman, E.; Lynn, M. J.; Xu, R.; Kaifer, A. E. *J. Am. Chem. Soc.* **1999**, *121*, 4304.
[27] Simard, J.; Briggs, C.; Boal, A. K.; Rotello, V. M. *Chem. Commun.* **2000**, 1943.
[28] Frankamp, B. L.; Uzun, O.; Ilhan, F.; Boal, A.; Rotello, V. M. *J. Am. Chem. Soc.* **2002**, *124*, 892.
[29] Kanehara, M.; Oumi, Y.; Sano, T.; Teranishi, T. *J. Am. Chem. Soc.* **2003**, *125*, 8708.
[30] Bowden, N. B.; Weck, M.; Choi, I. S.; Whitesides, G. M. *Acc. Chem. Res.* **2001**, *34*, 231.
[31] Dabbousi, B. O.; Murray, C. B.; Rubner, M. F.; Bawendi, M. G. *Chem. Mater.* **1994**, *6*, 216.
[32] Meldrum, F. C.; Kotov, N. A.; Fendler, J. H. *Chem. Mater.* **1995**, *7*, 1112.
[33] Brown, J. J.; Porter, J. A.; Daghlian, C. P.; Gibson, U. J. *Langmuir* **2001**, *17*, 7966.
[34] Murray, C. B.; Kagan, C. R.; Bawendi, M. G. *Science* **1995**, *270*, 1335.
[35] Thomas, P. J.; Kulkarni, G. U.; Rao, C. N. R. *J. Phys. Chem. B* **2001**, *105*, 2515.
[36] Talapin, D. V.; Shevchenko, E. V.; Kornowski, A.; Gaponik, N.; Haase, M.; Rogach, A. L.; Weller, H. *Adv. Mater.* **2001**, *13*, 1868.
[37] Harfenist, S. A.; Wang, Z. L.; Alvarez, M. M.; Vezmar, I.; Whetten, R. L. *J. Phys. Chem.* **1996**, *100*, 13904.
[38] Wang, Z. L.; Harfenist, S. A.; Vezmar, I.; Whetten, R. L.; Bentley, J.; Evans, N. D.; Alexander, K. B. *Adv. Mater.* **1998**, *10*, 808.
[39] Maye, M. M.; Zheng, W.; Leibowitz, F. L.; Ly, N. K.; Zhong, C. J. *Langmuir* **2000**, *16*, 490.
[40] Puntes, V. F.; Krishnan, K. M.; Alivisatos, P. *Appl. Phys. Lett.* **2001**, *78*, 2187.
[41] Lin, X. M.; Jaeger, H. M.; Sorensen, C. M.; Klabunde, K. J. *J. Phys. Chem. B* **2001**, *105*, 3353.
[42] Brown, L. O.; Hutchison, J. E. *J. Phys. Chem. B* **2001**, *105*, 8911.
[43] Yamamuro, S.; Farrell, D.; Humfeld, K. D.; Majetich, S. A. *MRS Symp. Proc.* **2001**, *636*, D108.
[44] Kondo, M.; Shinozaki, K.; Bergström, L.; Mizutani, N. *Langmuir* **1995**, *11*, 394.
[45] Goldenberg, L. M.; Wagner, J.; Stumpe, J.; Paulke, B. R.; Görnitz, E. *Langmuir* **2002**, *18*, 5627.
[46] Aoyama, Y.; Tanaka, Y.; Sugahara, S. *J. Am. Chem. Soc.* **1989**, *111*, 5397.
[47] Stavens, K. B.; Pusztay, S. V.; Zou, S.; Andres, R. P.; Wei, A. *Langmuir* **1999**, *15*, 8337.
[48] Balasubramanian, R.; Xu, J.; Kim, B.; Sadtler, B.; Wei, A. *J. Dispersion Sci. Technol.* **2001**, *22*, 485.
[49] Balasubramanian, R.; Kim, B.; Tripp, S. L.; Wang, X.; Lieberman, M.; Wei, A. *Langmuir* **2002**, *18*, 3676.
[50] Kim, B.; Tripp, S. L.; Wei, A. *J. Am. Chem. Soc.* **2001**, *123*, 7955.
[51] Wei, A.; Kim, B.; Pusztay, S. V.; Tripp, S. L.; Balasubramanian, R. *J. Inclusion Phenom. Macrocycl. Chem.* **2001**, *41*, 83.
[52] Kim, B.; Tripp, S. L.; Wei, A. *MRS Symp. Proc.* **2001**, *676*, Y61.
[53] Pusztay, S. V.; Wei, A.; Stavens, K. B.; Andres, R. P. *Supramol. Chem.* **2002**, *14*, 289.
[54] Tripp, S. L.; Pusztay, S. V.; Ribbe, A. E.; Wei, A. *J. Am. Chem. Soc.* **2002**, *124*, 7914.
[55] Tripp, S. L.; Dunin-Borkowski, R. E.; Wei, A. *Angew. Chem., Int. Ed. Engl.* **2003**, *42*, 5591.
[56] Kim, B.; Carignano, M. A.; Tripp, S. L.; Wei, A.*Langmuir*, **2004**, *20*, 9360.
[57] Pieranski, P. *Phys. Rev. Lett.* **1980**, *45*, 569.
[58] Beck, C.; Hartl, W.; Hempelmann, R. *Angew. Chem., Int. Ed. Engl.* **1999**, *38*, 1297.
[59] Hansen, P. H. F.; Bergström, L. *J. Colloid Interface Sci.* **1999**, *218*, 77.
[60] Hansen, P. H. F.; Malmsten, M.; Bergenståhl, B.; Bergström, L. *J. Colloid Interface Sci.* **1999**, *220*, 269.
[61] Spinner, E.; White, J. C. B. *J. Chem. Soc. B* **1966**, 991.
[62] Kobayashi, K.; Asakawa, Y.; Kato, Y.; Aoyama, Y. *J. Am. Chem. Soc.* **1992**, *114*, 10307.
[63] Gerkensmeier, T.; Mattay, J.; Näther, C. *Chem. Eur. J.* **2001**, *7*, 465.
[64] Boerrigter, H.; Verboom, W.; Reinhoudt, D. N. *J. Org. Chem.* **1997**, *62*, 7148.
[65] Román, E.; Peinador, C.; Mendoza, S.; Kaifer, A. E. *J. Org. Chem.* **1999**, *64*, 2577.